DUCTILITY OF REINFORCED CONCRETE MASONRY SHEAR WALLS UNDER SEISMIC LOADING

M. T. Shedid[1], R. G. Drysdale[2], and W. W. El-Dakhakhni[3]

[1] *Ph.D. Candidate, Dept. of Civil Engineering, McMaster University, Hamilton. Ontario, Canada*
[2] *Professor Emeritus, Dept. of Civil Engineering, McMaster University, Hamilton. Ontario, Canada*
[3] *Assistant Professor, Martini, Mascarin and George Chair in Masonry Design, Dept. of Civil Engineering, McMaster University, Hamilton. Ontario, Canada*
Email: shedidmmt@mcmaster.ca, drysdale@mcmaster.ca, eldak@mcmaster.ca

ABSTRACT:
The possibility of achieving a high level of ductility by flexural yielding in fully grouted reinforced concrete masonry shear walls is evaluated. Six full-scale walls were tested to failure under reversed cyclic lateral loading to investigate the effects of the amount and the distribution of vertical reinforcement and the level of axial compressive stress on the inelastic behavior and ductility of reinforced masonry shear walls. The test results indicated that the top wall displacement at the onset of yielding of the vertical reinforcement was highly dependent on the amount of reinforcement and minimally affected by the level of axial compressive load. However, at maximum lateral loads, the wall displacements were less sensitive to the amount of vertical reinforcement and to the level of axial compression. Correspondingly, the displacement ductility was found to be very sensitive to the amount of vertical reinforcement compared to the level of axial compression. In general, high levels of ductility accompanied by relatively small strength degradation were observed for the test specimens.

KEYWORDS: Masonry, Cyclic loads, Ductility, Shear walls, Concrete blocks

1. INTRODUCTION

The potential for major negative social and economic impact due to earthquake damage has led to adoption of more stringent seismic design requirements in North America, and in other parts of the world. In terms of potential damage, there is a perception that masonry structures do not have much ductility and are particularly vulnerable to seismic loading. However, this perception may be due to the lack of adequate data and some examples of failures of unreinforced or poorly constructed masonry structures. Therfore, there is a need for extensive research to document and evaluate the ductility of masonry shear walls.

The lack of sufficient data on earthquake resistance of reinforced masonry shear walls (RMSW) has led to several significant publications mentioned briefly below. Because shear failures of RMSW, characterized by diagonal tension cracking or sliding shear along mortar bed joints, are relatively brittle and exhibit comparatively rapid strength degradation after the ultimate load is reached, it is generally concurred that such failures should be avoided. The approach is to limit the lateral load (shear force) by ensuring that RMSW capacity is controlled by flexural yielding. Flexure controlled capacity is characterized by tensile yielding of the vertical reinforcement, formation of a plastic hinge zone at the bottom of the wall and, eventually, compression crushing of the masonry. This favored failure mode provides ductility and is effective in dissipating energy by yielding of the vertical reinforcement and inelastic deformation of the masonry. The flexural capacity of RMSW is easily calculated with a reasonable degree of accuracy (Priestley 1986; Shing et al. 1989). However, the ductility and energy dissipation capabilities of such walls are not well quantified, despite being key factors in predicting the structural performance under earthquake loading.

In the current study, the behavior for six fully grouted RMSW tested with different amounts of flexural reinforcement and axial compression is reported. The aim of the study was to document and evaluate the effects of these parameters to facilitate better understanding of the inelastic behavior under seismic loading.

2. EXPERIMENTAL PROGRAM

The experimental program consisted of testing 6 RMSW, having four different amounts and two distributions of vertical reinforcement and being subjected to three different levels of axial compressive stress to document the effect of these parameters on the flexural behavior of RMSW. All walls were subjected to fully reversed displacement- controlled quasi-static cyclic loading and were cycled up to 50% degradation in strength to obtain information about the post-peak behavior.

2.1. Material Properties

The compressive strengths of the hollow 20 cm blocks used in wall construction, based on average net area of the block, were 24.8 MPa and 20.5 MPa, for Stretcher and Splitter units, respectively. Type S mortar, with an average flow of 125% was batched by weight with proportions of Portland cement: Lime: Dry sand: Water = 1.0: 0.2: 3.5: 0.9. Tests of twenty randomly selected mortar cubes resulted in an average compressive strength of 27.7 MPa (*c.o.v. = 11.6%)*. Premixed fine grout, having 254 mm slump, was used for grouting the walls. The average block molded compressive strength of the grout used was 36.5 MPa (*c.o.v. = 8.6%)*.

Grout filled 4-block high prisms were constructed in running bond to determine the wall properties. The average compressive strength of the grouted prisms, f'_m, was 14.8 MPa (*c.o.v. = 4.4%)*. In accordance with CSA S304.1 (2004), this value would be the basis for choosing design strength values, whereas for the MSJC code (2005), where 2-block high prisms (height to thickness ratio of 2) are considered to represent masonry compressive strength in the wall, the 4 block high prism results would be modified to be $14.8 \times 1.15 = 17.0$ MPa.

The concrete used in the wall foundation had an average compressive strength of 39.8 MPa (*c.o.v* = 1.8%). Tensile tests were conducted on the reinforcement used for all walls. The average yield strength for the vertical reinforcement used in all walls was 502 MPa (*c.o.v* = 0.6%) except for the vertical reinforcement used in Wall 6, which was obtained separately and had an unexpected yield strength of 624 MPa (about 24 % higher than for the other walls). The average yield strength for the horizontal reinforcement was 491 MPa (*c.o.v* = 0.4%).

2.2. Wall Design and Construction

To achieve flexure dominated behavior with a distinct region of plastic hinging, it was decided that the aspect ratio of the test walls (height/length) should be at least 2.0. The second criterion in selecting the wall dimensions was to ensure that the compression zone length at ultimate load was greater than one block long (400 mm) in order to have more than one grouted cell and bar in compression. Calculations based on beam theory showed that the minimum wall length should be 1.6 m (4 blocks long) in order to have at least one block under compression. Finally, to allow for various symmetrical distributions of vertical reinforcement in the wall such as having a bar in every cell, every other cell, and every fourth cell, wall length, l_w, was selected to be 1.8 m (4.5 blocks long, containing 9 cells). Consequently, a wall height, h_w, of 3.6 m was selected to achieve the aspect ratio of 2.0.

A standard 2-cell hollow 20 cm concrete masonry block (190 × 190 × 390 mm) which is similar to the 8 in block commonly used in the USA was selected. Each course of the 1.8 m long wall was constructed using four and half masonry units. The shear reinforcement was a single leg No. 10 bar (100 mm^2 area) with a 350 mm long 180-degree hook around the outermost vertical bar located at 100 mm from each end of the wall. The webs of the blocks in courses containing horizontal reinforcement were saw cut and knocked-out to a depth of 90 mm to form a larger continuous horizontal cell or bond beam that accommodated the shear reinforcement and provided full embedment in the grout. To provide a fixed base for the walls, the vertical reinforcement was anchored in a reinforced concrete foundation. The bars terminated with a 90° hook and were tied to longitudinal bars in the wall foundation to help maintain accurate bar position during pouring of the concrete. The vertical reinforcement for the wall extended to the full height of the wall without splicing in order to eliminate difficulty with interpretation of test results when splice lengths are included.

The walls were constructed by an experienced mason in a standard running bond pattern using face shell mortar bedding and 10 mm mortar joints. A summary of the vertical and the horizontal reinforcement arrangements and the levels of axial compressive stress for the test walls is given in Table 2.1. The vertical and horizontal reinforcement ratios, ρ_v and ρ_h, are defined as ratios of the areas of reinforcing bars to gross area of the horizontal or vertical masonry cross section, respectively. Walls 1 and 4 had the lowest and the highest amounts of vertical reinforcement, respectively. Wall 3 had the vertical reinforcement (5 No. 25) placed in every other cell, whereas, Wall 2, with almost the same vertical steel ratio, had the vertical reinforcement (9 No. 20) placed in every cell. Walls 5 and 6 were the same as Wall 4 with the highest amount of vertical reinforcement (9 No. 25), but were subjected to axial compressive stresses of about 0.05 f'_m and 0.10 f'_m (i.e., 0.75 MPa and 1.50 MPa), respectively. All walls were designed to exhibit ductile flexural failure by providing sufficient horizontal reinforcement in accordance with CSA S304.1 (2004) and the MSJC code (2005) to safeguard against shear failure. The wall types according to the MSJC code (2005) are listed in Table 2.1.

Table 2.1: Summary of wall details

Wall	Vertical reinforcement		Horizontal reinforcement		Axial compressive stress (MPa)	MSJC (2005) wall types
	No. and size	ρ_v (%)	No. and spacing	ρ_h (%)		
1	5 No. 15 (200 mm^2)	0.29	No.10 bars @ 600 mm	0.08	0	Special
2	9 No.20 (300 mm^2)	0.78	No.10 bars @ 400 mm	0.13	0	Intermediate
3	5 No.25 (500 mm^2)	0.73	No.10 bars @ 400 mm	0.13	0	Intermediate
4	9 No.25 (500 mm^2)	1.31	No.10 bars @ 200 mm	1.13	0	Ordinary
5	9 No.25 (500 mm^2)	1.31	No.10 bars @ 200 mm	0.26	0.75	Ordinary
6	9 No.25 (500 mm^2)	1.31	No.10 bars @ 200 mm	0.26	1.50	Ordinary

2.3. Test Setup and Instrumentation

Figure 1 shows the test setup with the wall foundation prestressed onto a larger reinforced concrete slab which was, in turn, prestressed to the structural floor of the laboratory. At the top of the wall, the vertical reinforcement extended through and was welded to a U-shaped built-up steel loading beam. This was intended to simulate a rigid diaphragm and provide uniform transmission of horizontal load to the shear wall instead of a concentrated load at the upper end of the wall. The lateral load was supplied though a displacement controlled 1,400 kN hydraulic actuator with its centerline aligned with the top of the wall. Rollers were attached to the out-of-plane bracing in order to prevent out-of-plane displacement while providing no resistance to in-plane displacement. Axial load was applied using a manually controlled jack using 2 sets of 2 steel rods located at both sides of the wall.

During testing, loads, displacements and strains were recorded using a computerized data acquisition system. As shown in Fig. 1, 29 displacement potentiometers were used to monitor the vertical, horizontal and diagonal displacements of the masonry as well as the slip with respect to the wall foundation. Lateral displacements relative to the wall foundation were measured using potentiometers attached at eight different heights to a truss system which was supported on the wall foundation. Vertical displacements with respect to the wall foundation were measured using 7 potentiometers at each wall end installed vertically over the wall height. Also, 10 strain gauges were attached to the outermost reinforcing bars within the most highly stressed region to investigate the extent of yielding over the wall height and inside the concrete foundation, as well as identifying the displacement at the onset of yielding of the outermost reinforcement.

The cyclic loading scheme adopted for all tests consisted of a series of displacement-controlled loading cycles to assess the strength and the stiffness degradation at each displacement level. The walls were cycled twice at each displacement level. To obtain information that included the post-peak behavior, displacements were increase incrementally until the specimen had achieved maximum lateral load resistance and then lost up to about 50% of its maximum capacity.

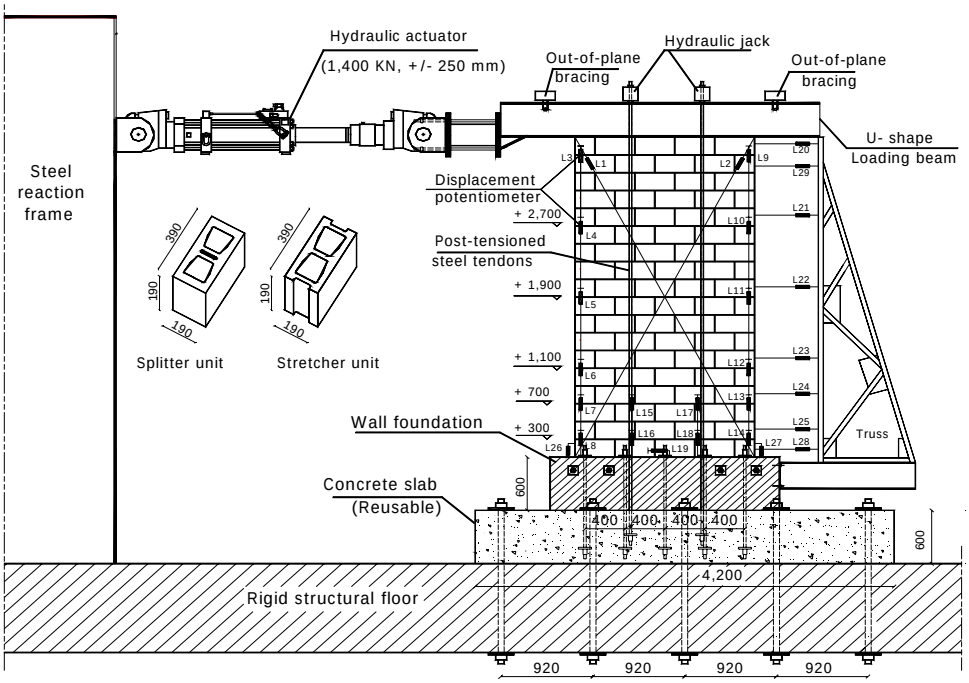

Figure 1 Test setup

3. EXPERIMENTAL RESULTS

All the test walls exhibited a reasonably symmetric load-displacement relationship for loading in both directions until toe crushing occurred at one end. After reaching the maximum load, and even considering the somewhat different damage levels in the crushed toes at either end of a wall, degradation in strength was remarkably similar up to very large displacements. The behavior of all walls was dominated by a flexural response as evident by horizontal cracking along the bed joints and yielding of the vertical reinforcement observed over the lower courses of the walls even at low displacement levels as shown in Fig. 2(a). Under increased displacement, stepped cracks, passing through the mortar joints, started to form over the middle third region of the wall height and were accompanied by extension of the horizontal cracks towards the midlength of the wall [Fig. 2(b)]. With further increasing displacements, stepped cracks extended to the top and bottom of the walls and were accompanied by diagonal cracks crossing through the grout filled blocks [Fig. 2(c)].

As loading continued, vertical splitting cracks typically appeared in the wall toes under compression [Fig. 2(d)] and extended to the courses above the wall foundation. Whereas, wide horizontal bed joint cracks were clearly visible at the wall end subjected to tensile stresses. Inclined cracks later formed in the face shells at the compression toe and, along with the vertical splitting cracks, resulted in significant damage at the wall toes. After toe crushing and face shell spalling at the wall toes, it was possible to see the outermost grout columns which were almost intact except for some vertical cracks [Fig. 2(e)].

With increased displacement, spalling of the face shell and grout cracking became more significant at the compression end of the wall. Widening of the vertical crack in the grout column coincided with initial buckling of the vertical reinforcement in the outermost cell and between the horizontal reinforcement. Further splitting and eventually crumbling of the outermost grout column [Fig. 2(f)] in the compression end occurred along the buckled length of the vertical reinforcement. Although the buckled bar straightened up under tension during the reversed load cycle, degradation of the lateral resistance was more pronounced after buckling of the vertical reinforcement had occurred, especially for walls subjected to axial compression. Various damage levels were observed at the end of the test for each wall depending on the reinforcement ratio and axial stress. Additional details of the test matrix, behaviors of individual walls, and failure modes, were presented by Shedid (2006).

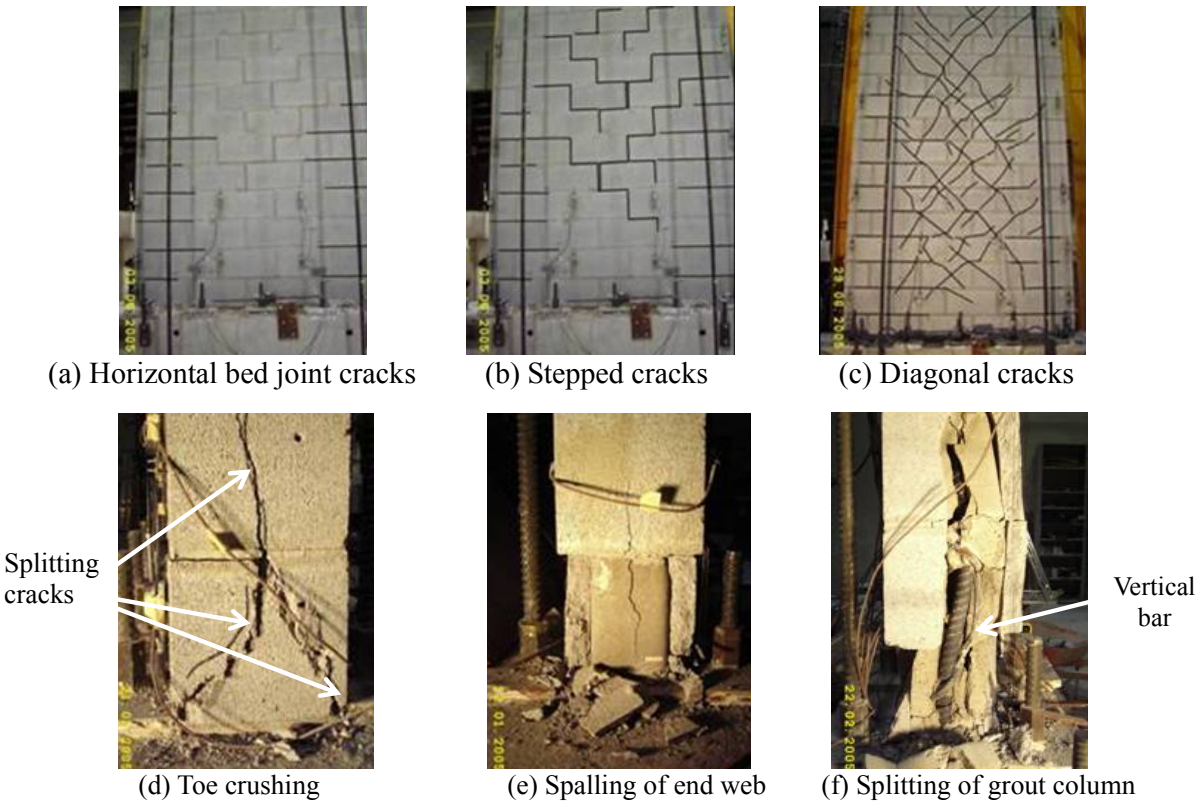

Figure 2 Typical progression of cracking documented for various walls

3.1 Load-Displacement Relationships

The load-displacement relationships for selected walls with the extremes of reinforcement are presented in Fig. 3. The lateral forces corresponding to the onset of yield of the outermost bar and to the ultimate flexural capacity are designated as Q_y and Q_u, respectively. Lateral displacements are indicated as absolute values and as multiples of the yield displacement, Δ_y, corresponding to the displacement ductility at that point defined as $\mu_\Delta = \Delta/\Delta_y$. The top displacement is also shown in terms of percent drift ($\Delta \times 100/3600$).

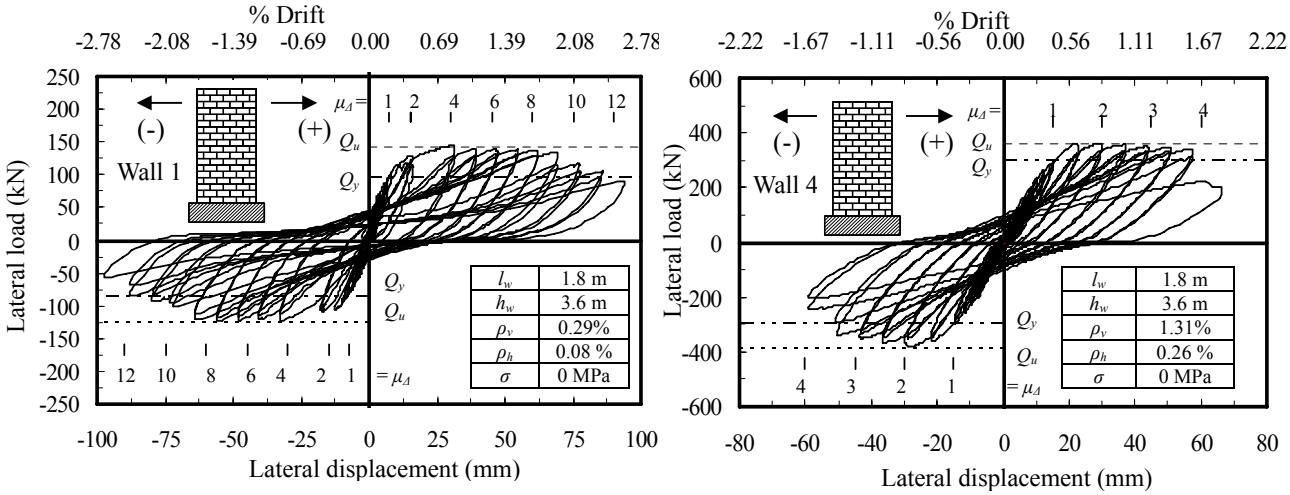

Figure 3 Hysteresis loops

All walls behaved in an almost linearly elastic manner up to the onset of yield of the outermost bar. This resulted in thin hysteresis loops which are characterized by low energy dissipation. At higher displacement levels, the area within the hysteresis loops increased indicating higher levels of energy dissipation as a result of increased inelastic deformation and the level of damage. For loading beyond the initial yield displacement, the second cycle of loading produced less resistance corresponding to the same displacement, which can be attributes to the reduction in the reloading stiffness. However, as can be seen, increasing the displacement to the next increment consistently resulted in regaining the previous resistance up to the displacement at which very significant damage was clearly visible.

The effects of the amount of vertical reinforcement and the level of the axial compressive stress on the response of the test walls are shown in Figs. 4 (a) and (b), respectively. In this figure, the load-displacement data for Wall 6 was adjusted to account for the effect of the aforementioned higher yield strength of the reinforcement used (24% higher than all other walls). Wall capacity calculations at the onset of yield and at ultimate load showed that a 24% increase of the yield strength of the vertical reinforcement would increase the wall capacity, on average, by about 11%.]Note that axial compression had a significant effect on flexural capacity]. Therefore, the resistance for Wall 6 in the load-displacement diagram was multiplied by a factor of 0.89 to make the comparison between the walls more meaningful. Contrary to the common perception, the graphs in Fig. 4 show quite ductile behavior for all walls characterized by relatively small strength degradation with increased displacement after reaching maximum loads. Walls 5 and 6, with axial compressive stresses and very high vertical reinforcement ratios, experienced more distinct strength degradation and less ductility compared to Walls 1, 2, 3, and 4 with equal or lesser amounts of vertical reinforcement and no axial compressive stress.

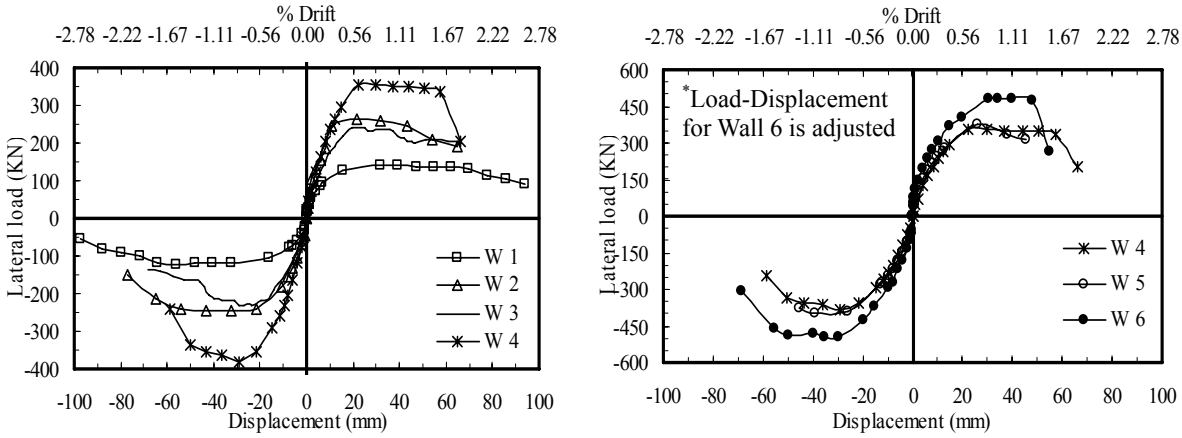

(a) Effect of amount of reinforcement (b) Effect of axial load

Figure 4 Effect of the amount of reinforcement and level of axial load on wall response

3.2 Deformation Profile along the Wall Height

As can be seen in Fig. 5, concentration of rotation over the lower part of the wall is evident whereas, the deformation over the top portion of the wall tended to be very small. This indicates that most of the plastic deformation occurs close to the base of the walls and that the top part of the wall behaved as a rigid body.

3.4 Displacement Characteristics

Figure 6 (a) shows the effects of vertical reinforcement ratio on the lateral displacement at the onset of yield of the outermost bar, at maximum load, and at 20% strength degradation for both directions of loading. The measured displacement at first yield, Δ_y, almost doubled corresponding to an increase of the amount of reinforcement from 0.29% to 1.31%. Also Δ_y tended to slightly increase with increases of the axial compressive stress as shown in Fig. 6 (b). A 12% increase in Δ_y was recorded corresponding to an increase in axial stress from 0.0 to 1.5 MPa, when comparing the results of Walls 4 and 6, respectively. For all walls, the ultimate capacity was reached at a top

displacement of approximately 30 mm (0.83 % drift). This shows that Δ_u is not very sensitive to the amount or distribution of the vertical reinforcement or the level of axial load. Comparing $\Delta_{0.80u}$ and Δ_u values, it can be seen that all walls retained 80% of their ultimate capacities at displacements well exceeding 1% drift.

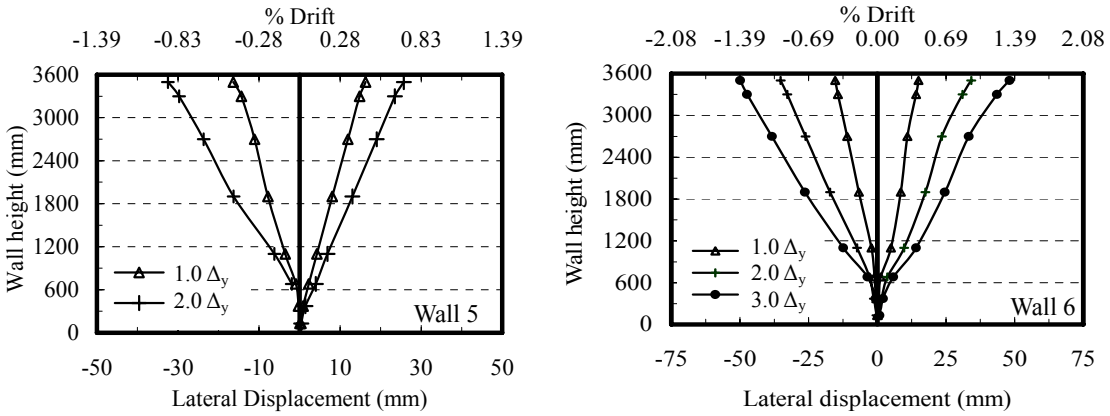

Figure 5 Deflection profile along the wall height

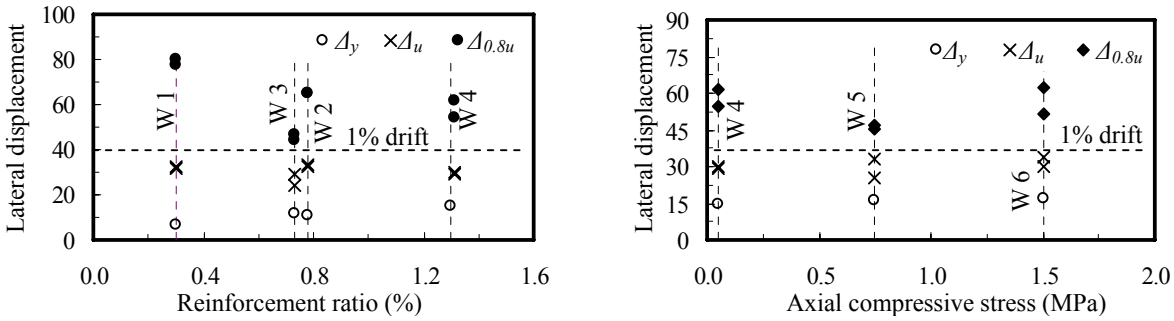

(a) Effect of amount of reinforcement (b) Effect of axial load

Figure 6 Effect of steel ratio and axial stress on lateral displacement

3.5 Displacement Ductility

Ductility is a measure of the ability of the wall to deform beyond yielding of the flexural reinforcement. The displacement ductility, μ_Δ, is defined herein as the ratio between the top displacement and the displacement at the onset of yield of the outermost vertical bar. There are several discussions in the literature regarding the appropriate definition of displacement ductility, but, as indicated by Priestley (2000), there is no general consensus or a unified definition for the yield and the ultimate displacements. Many researchers (Park and Paulay 1975, Priestley et al. 1996, Tomazevic 1998) have proposed to evaluate the displacement ductility using an equivalent elastic-perfectly plastic system, but different methods were presented to define the equivalent system. The aim of this study is to document experimental results related to wall ductility, therefore, the experimental values of displacements are used without idealizing the load-displacement relationships to an elasto-plastic system.

As shown in Fig. 7, displacement ductility values at maximum load, calculated with respect to the displacement at first yield of the outermost reinforcement, ranged from 1.7 for a heavily reinforced highly stressed wall to 4.5 for a lightly reinforced wall not axially stressed, and ranged between 3.3 to 11.4 after 20% strength degradation. Relatively lower drifts corresponding to 20% strength degradation were measured for Walls 3 and 5 compared to the rest of the walls. For Wall 3, high sliding displacements were recorded associated with a continuous wide crack between the wall and the wall foundation. These sliding displacements may have led to a rapid strength degradation leading to a lower value for $\mu_{\Delta 0.8u}$. For Wall 5, a severe twist, which occurred during testing, led to deterioration of the wall face shells on one side of the wall close to maximum load and resulted in an early loss of lateral strength resulting in a decreased displacement ductility value at 20% strength degradation.

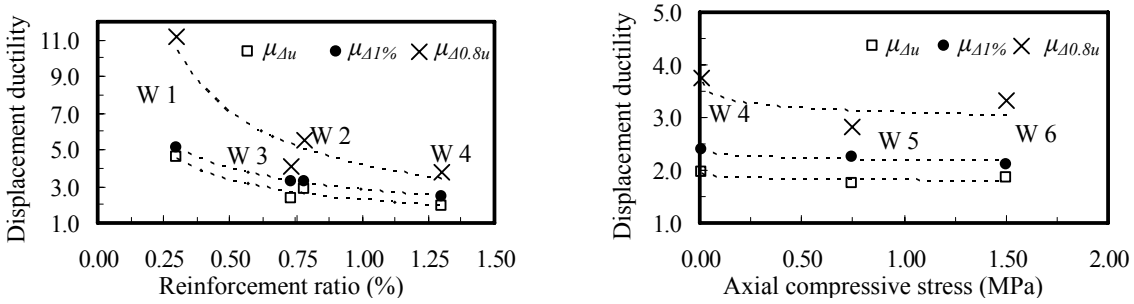

Figure 7 Effect of steel ratio and axial stress on displacement ductility

4. CONCLUSION

All walls exhibited reasonably symmetric behavior in both directions of loading until toe crushing occurred.
The behavior of the walls was characterized by concentration of rotation over the lower part of the wall whereas, the top part of the wall deformed as a rigid body.
The test results showed that the yield displacement tended to increase with increases in the vertical reinforcement ratio and the axial compressive stress. It was also observed that all the test walls (with an aspect ratio of 2.0) reached their maximum capacity at top displacements close to 30 mm (0.83% Drift) regardless of the test parameters.
The displacement ductility decreased with increasing amounts of vertical reinforcement and increasing axial compressive stress. The displacement ductilities corresponding to 20% degradation in strength are significantly higher than the displacement ductilities corresponding to maximum load.
Contrary to the common perception that masonry walls are not ductile, the test results showed that reinforced masonry shear walls failing in flexure behave in an obviously ductile manner with little strength degradation up to and beyond usable drift levels.

5. ACKNOWLEDGMENT

The financial support of the McMaster University Centre for Effective Design of Structures (*CEDS*) funded through the Ontario Research and Development Challenge Fund (*ORDCF*) is greatly appreciated. Provision of mason time by Ontario Masonry Contractors Association and Canada Masonry Design Centre is appreciated. The supply of concrete blocks and grout by Boehmer Block Ltd. is gratefully acknowledged.

6. REFERENCES

Canadian Standards Association (CSA 2004). Design of masonry structures. CSA S304.1-04, Ontario, Canada.
Masonry Standards Joint Committee (MSJC 2005). Building code requirements for Masonry Structures. ACI 530/ASCE 5 /TMS 402, American Concrete Institute, American Society of Civil Engineers, and The Masonry Society, Detroit, New York, and Boulder.
Park, R. and Paulay, T. (1975). Reinforced concrete structures. John Wiley and Sons, Inc., New York.
Priestley, M. (1986). "Seismic design of concrete masonry shear walls." *American Concrete Institute Structural Journal*, **(83)1**, 58-68.
Priestley, M., Seible, F., and Calvi, G. (1996). Seismic design and retrofit of bridges. John Wiley and Sons, N.Y.
Priestley, M. (2000). Performance based seismic design. Proceedings 12th World Conference Earthquake Engineering.
Shedid, M. (2006). "Ductility of reinforced concrete masonry shear walls." M.A.Sc. Thesis, Department of Civil Engineering, McMaster University, Ontario, Canada.
Shing, P., Noland, J., Klamerus, E., and Spaeh., H. (1989). Inelastic behavior of concrete masonry shear walls. *J. Struct. Eng*., **(115)9**, 2204-2225.
Tomazevic, M. (1998). Earthquake-Resistant Design of Masonry Buildings. Imperial College Press, Covent Garden, London, UK.